Cross Section for "Ultracold" Neutrons

I. Theory of Magnetic Scattering

K. BINDER

Physikdepartment E 14, Technische Universität München

(Z. Naturforsch. **26 a**, 432—441 [1971]; eingegangen am 19. November 1970)

Dedicated to Prof. H. Maier-Leibnitz on his 60th birthday

Very cold neutrons (typical wavelengths are about 10^2 Å) are available by recently developed techniques [1, 2]. The features of the scattering of these "ultracold" neutrons are investigated in the present paper discussing a few examples of magnetic scattering. The diffraction of neutrons by the vortex lattice in superconductors is treated as an example of elastic scattering, while in most other cases the scattering is inelastic. We discuss the scattering by ferromagnetic magnons at low temperatures and the critical scattering from an isotropic ferromagnet above the critical temperature. Simple models are used to derive the total cross sections. It is shown that relevant information about the inealsticity can be gained by the measurement of total cross sections in these cases.

1. Introduction

We use the notation "ultracold neutrons" [3] for neutrons with wavelengths (considerably) larger than 20 Å. Small amounts of such neutrons can be found within the thermal spectrum of reactors. Methods have been proposed and developed to extract these neutrons from the thermal spectrum [1–4]. With the apparatus at the FRM reactor neutrons can be observed with wavelengths between about 40 Å and 1000 Å. The latter value corresponds to a neutron energy of about 10^{-7} eV. It has been proposed [5] to measure the electric dipole moment of the neutron using ultracold neutrons, since it seems possible to achieve a higher accuracy than in previous experiments (e. g. [6]). It is clear that it would be very interesting also to measure the scattering of neutrons with similarly small energy transfers; information about such energy levels of the scatterer could be obtained which cannot be investigated by thermal neutron scattering.

The theory of the scattering cross sections for thermal neutrons has been investigated in great detail (e. g. [7–9]). Little information can be taken from the literature about the cross section of very cold neutrons, however. Therefore the present paper gives a crude survey about the magnetic scattering cross sections of ultracold neutrons. The diffraction of neutrons by the vortex lattice in the mixed state of type-II-superconductors serves as a simple example of elastic scattering. Two examples of inelastic magnetic scattering are treated, the scattering by ferromagnetic spin waves at low temperatures and the critical scattering from an isotropic ferromagnet above the critical temperature. We use rather crude models for the inelasticity of the scattering to derive a simple description of the total cross sections. The main experimental interest concerns the total cross section at the present time, since the available intensities are not yet very high. At the FRM reactor the intensity of neutrons with a velocity $v = 90$ m/sec (corresponding wavelength $\lambda \approx 45$ Å), resolution $\Delta v/v \approx 7.4\%$ is $F.\ \Phi = 1200$ neutrons/sec [2] the area being $F = 6\ \text{cm}^2$, and the flux Φ varies approximately as v^3 [1]. Thus we do not discuss the indicated possibility of investigating the energy distribution of the scattered neutrons further. We show, however, that some relevant information about the inelasticity of the scattering can be gained also by the measurement of total cross sections, if

Reprints request to Dr. H. VONACH, Physik-Department E 14 der Technischen Hochschule München, *D-8000 München 2*, Arcisstraße 21.

1 A. STEYERL, Phys. Lett. **29 B**, 33 [1969].
2 A. STEYERL, to be published.
3 V. I. LUSHCHIKOV, YU. N. POKOTILOSKII, A. V. STRELKOV, and F. L. SHAPIRO, Zh. ETF Pis. Red. **9**, 40 [1969].
4 H. MAIER-LEIBNITZ and A. STEYERL, in: Konferenzbericht Diskussionstagung Neutronenphysik an Forschungsreaktoren, April ,25—28, 1967, Jülich, p. 217.
5 F. L. SHAPIRO, Soviet Phys. Uspekhi **11**, 345 [1968].
6 J. SMITH, E. PURCELL, and N. RAMSEY, Phys. Rev. **108**, 120 [1957].
7 P. A. EGELSTAFF, Thermal Neutron Scattering, Academic Press, New York and London 1965.
8 V. F. TURCHIN, Slow Neutrons, Isr. Progr. f. Sc. Transl. Jerusalem 1965.
9 I. I. GUREVICH and L. V. TARASOV, Low Energy Neutron Physics, North Holland Publ. Comp., Amsterdam 1968.

suitable models are used to analyze the cross sections. In a second paper of this series we intend to present some examples of nuclear inelastic scattering from solids, liquids and gases.

2. Bragg Scattering of Ultracold Neutrons from the Vortex Lattice in Superconductors

Elastic scattering of ultracold neutrons will be important, if the structures of the scatterer have a linear dimension comparable to the neutron wavelength. If a type II-superconductor is brought into a magnetic field, the magnetic flux enters the superconductor in its mixed state as flux lines which form a regular array [10]. The lattice spacing δ has the order of magnitude of 10^3 Å. Each vortex line carries a flux quantum $\Phi_0 = c\,h/2\,e = 2.10^{-7}$ Gauss cm^2, c being the velocity of light, h the Planck's constant and e the charge of the electron. Within each vortex line of radius ξ the substance is in its normal state, while outside of the flux line the magnetic induction decreases. The penetration depth of the magnetic field is characterized by the parameter λ_p. The distribution of the magnetic field outside of the flux lines can be found from the Ginzburg-Landau equations in the limiting case [10] $\xi = 0$. The fourier transform of the magnetic moment distribution acts as the magnetic form factor of the scattering. It is easy to derive the extinction coefficient in this case [11]

$$\Sigma = \frac{m^2}{\hbar^4\,k^2}\,(\gamma\,\mu_N\,B)^2 \cdot \sum_{\tau \neq 0}^{\tau \leq 2k} \frac{1}{\tau\,\sqrt{1-(\tau/2\,k)^2}\,(1+\tau^2\,\lambda_p^2)^2}\,, \tag{1}$$

m neutron mass, $k = 2\,\pi/\lambda$ neutron wave number, μ_N nuclear magneton $\gamma = 1.91$, B magnetic induction.

The vectors of the reciprocal lattice τ can be expressed in terms of the magnetic induction and the flux quantum. Since the flux lines form a triangular lattice we can write

$$\tau = 2\,\pi\,\sqrt{2\,B(K^2+L^2-K\,L)/(\sqrt{3}\,\Phi_0)}\,. \tag{2}$$

$K, L = 0, \pm 1, \pm 2, \ldots$ integer numbers.

We take $\lambda_p = 400$ Å (the value of Nb [12]) to evaluate Eqs. (1), (2) numerically. It is not possible to neglect ξ in comparison to λ_p in the case of Nb, however; it is well known that in the case $\xi \approx \lambda_p$ a quasisinoidal distribution of the magnetic induction results [12]. A magnetic form factor as given by Eq. (1) is a bad description in this case; we believe, however, that Eq. (1) will be a useful description for some other substances having smaller values of ξ. The cross section is plotted versus the energy E of the neutrons in Fig. 1 for three values of the magnetic induction B. The large values of the cross section are very remarkable. Since impurities, lattice defects etc. are known to act as pinning centers [13] to the vortex lattice, distortions of the flux

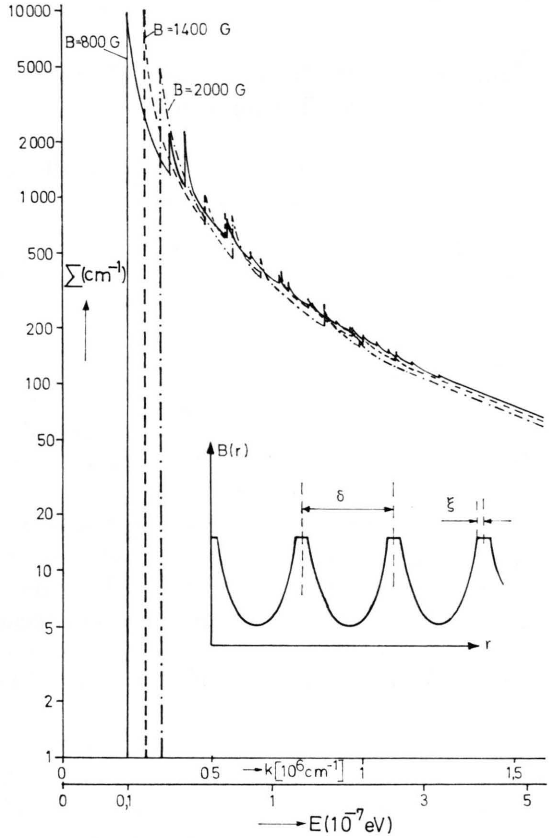

Fig. 1. Cross section of type II-superconductor plotted versus the neutron wave number k or neutron energy E, respectively. Three values of magnetic induction B have been chosen. The magnetic induction in the superconductor is plotted versus the distance schematically in the lower part of the figure. The distance between two vortex lines is denoted by δ, the radius of a vortex line is denoted by ξ.

[10] A. A. ABRIKOSOV, Soviet Phys. JETP **5**, 1174 [1957].
[11] M. P. KEMOKLIDZE, Soviet Phys. JETP **20**, 1505 [1965].
[12] D. CRIBIER, B. JACROT, L. MADHAV RAO, and B. FARNOUX, Progr. in Low Tem. Phys. **5**, 161 [1967].
[13] J. FRIEDEL, P. G. DE GENNES, and J. MATRICON, Appl. Phys. Lett. **2**, 119 [1963].

lattice can occur [14]. The discontinuities of the neutron cross section will be smeared out by the lattice distortions, and the magnitude of the cross section is reduced. A second effect which can reduce the intensity is the variation of the magnitude of the lattice spacing through the sample — this effect has been observed in some cases by means of the Bitter technique [15]. In the experiments by CRIBIER et al. [12] using cold neutrons ($\lambda \approx 5$ Å) the Bragg angle has a magnitude of minutes of arc. Using ultracold neutrons large Bragg angles could be obtained, and the intensity of the first Bragg peak would be high. The cross section and the intensity decrease with neutron energy E according to a $1/E$-law.

3. Spin-wave Scattering of Ultracold Neutrons at Low Temperatures

The differential cross sections for the scattering of neutrons with absorption or emission of a spin-wave are given by [16–18]

$$\left(\frac{d^2\sigma}{d\Omega\, d\omega}\right)_{\substack{\text{abs}\\ \text{em}}} = (r_0\,\gamma)^2 \,|F(\boldsymbol{q})|^2 \frac{k'}{k}\frac{S}{2} \cdot [1+(\boldsymbol{e}\,\boldsymbol{\mu})^2]\frac{(2\pi)^3}{V_0}\sum_\tau \sum_f \delta(\omega \mp \omega_f) \cdot \delta(\boldsymbol{q} \pm \boldsymbol{f} - \boldsymbol{\tau})\left[\frac{1}{\exp\{\hbar\,\omega_f/k_B T\}-1} + \frac{1}{2} \pm \frac{1}{2}\right]. \tag{3}$$

$\boldsymbol{q} = \boldsymbol{k}' - \boldsymbol{k}$ scattering vector, $\boldsymbol{e} = \boldsymbol{q}/|\boldsymbol{q}|$, $\hbar\,\boldsymbol{k}'$ momentum of the scattered neutron, r_0 radius of the electron, $\hbar\,\omega$ energy transfer, $|F(\boldsymbol{q})|^2$ magnetic form factor, S spin quantum number, $\boldsymbol{\mu}$ unit vector in the direction of the magnetization, V_0 volume of the elementary cell, k_B Boltzmann's constant, T temperature.

Eq. (3) applies to spin waves with momentum $\hbar\,\boldsymbol{f}$ and energy $\hbar\,\omega_f$; the finite linewidth of the magnons can be neglected since we consider only temperatures $T \ll T_c$. We want to include a small anisotropy into our treatment; we do not use the HOLSTEIN-PRIMAKOFF [19] dispersion relation for the spin waves but rather represent the anisotropy by some "effective field" H_a and get

$$\hbar\,\omega_f = g\,\mu_0\,H_a + 2\,S\sum_R I_{0R}(1-\exp\{i\,\boldsymbol{f}\,\boldsymbol{R}\}) \underset{\text{small } f}{\approx} g\,\mu_0\,H_a + 2\,S\,I\,d^2 f^2 = E_A + \hbar^2 f^2/2\,m^*. \tag{4}$$

μ_0 Bohr's magneton, g splitting factor, $I_{0R} = I$ exchange constant between nearest neighbors, d lattice spacing, m^* "effective mass" of the magnon.

The ratio neutron mass to magnon mass has a value of about 10^2 for typical ferromagnets as Fe or Ni; we shall consider mainly ferromagnets with low Curie temperatures T_c permitting small values of m/m^*. Averaging over the directions of $\boldsymbol{\mu}$ and integrating over the energy transfer ω we find

$$\left(\frac{d\Omega}{d\sigma}\right)_{\text{abs}} = \frac{2\,S}{3}(r_0\,\gamma)^2\frac{|F(\boldsymbol{q})|^2}{k}\sum_\tau{}' \cdot \sqrt{k^2 + \frac{2\,m}{\hbar}\,\omega_{\boldsymbol{\tau}-\boldsymbol{q}}}\;\frac{1}{\exp\{\hbar\,\omega_{\boldsymbol{\tau}-\boldsymbol{q}}/k_B T\}-1} \tag{5}$$

and

$$\left(\frac{d\sigma}{d\Omega}\right)_{\text{em}} = \frac{2\,S}{3}(r_0\,\gamma)^2\frac{|F(\boldsymbol{q})|^2}{k}\sum_\tau{}' \cdot \sqrt{k^2 - \frac{2\,m}{\hbar}\,\omega_{\boldsymbol{\tau}-\boldsymbol{q}}}\left[\frac{1}{\exp\{\hbar\,\omega_{\boldsymbol{\tau}-\boldsymbol{q}}/k_B T\}-1} + 1\right]. \tag{6}$$

The sum $\sum_f$ was replaced by an integral to derive Eqs. (5), (6). The primes in the sums $\sum_\tau$ mean that the sums have to be extended over such reciprocal lattice vectors only that $\boldsymbol{k} = \boldsymbol{\tau} - \boldsymbol{q}$ lies within the first Brillouin zone. If $m/m^* < \pi^2/2$ we have only a contribution of $\tau = 0$ in the sums when $k \to 0$, while some contributions to the magnon absorption cross section with $\tau \neq 0$ can occur for larger m/m^* in the limit $k \to 0$.

We can give a rough estimate for such contributions by

$$\sigma_\tau \approx \frac{4\,\pi}{3}\,S(r_0\,\gamma)^2\,|F(\boldsymbol{\tau})|^2(\tau/k)\,(m^*/m)^{3/2} \cdot 1/[\exp\{\hbar^2\,\tau^2/2\,m\,k_B T\}-1]\,. \tag{7}$$

These contributions vary with the neutron velocity v as $1/v$ and cannot be separated from the nuclear absorption σ_a experimentally, since σ_τ will always be some orders of magnitude smaller than σ_a. A different behavior is found for the contributions of

[14] W. A. FIETZ and W. W. WEBB, Phys. Rev. **178**, 657 [1969].
[15] H. TRÄUBLE and U. ESSMANN, Phys. Stat. Sol. **25**, 373 [1968].
[16] YU. A. IZYUMOV, Soviet Phys. Uspekhi **16**, 359 [1963].
[17] S. V. MALEEV, Soviet Phys. JETP **6**, 776 [1958].
[18] R. J. ELLIOTT and R. D. LOWDE, Proc. Roy. Soc. London **230**, 46 [1955].
[19] T. HOLSTEIN and H. PRIMAKOFF, Phys. Rev. **58**, 1098 [1940].

$\tau = 0$, however. It is easy to show that scattering with magnon absorption and emission can occur only if the inequalities

$$\frac{E_A}{E}\left(\frac{m}{m^*}-1\right) \leqq 1\,, \quad \frac{E_A}{E}\left(\frac{m}{m^*}+1\right) \leqq 1$$

respectively, are fulfilled. We now restrict our interest to small values of E_A and not to large m/m^*; in this case the two limiting energies will be in the energy region of the ultracold neutrons. Using the quadratic dispersion law Eq. (4) and expanding the denominators in Eq. (5), (6) we can perform the angular integration to derive the total cross section by making use of the relation

$$q^2 = k^2 + \left(k^2 \pm \frac{2\,m}{\hbar}\,\omega_q\right) - 2\,k\sqrt{k^2 \pm \frac{2\,m}{\hbar}\,\omega_q}\,\cos\vartheta \tag{8}$$

[scattering angle ϑ ($\pm$ refers to magnon absorption and emission, respectively)] and get ($k_B\,T \gg E_A$)

$$\sigma_{\rm abs} \approx \frac{\pi}{3}(r_0\,\gamma)^2\,S\left(\frac{m^*}{m}\right)\frac{k_B\,T}{E_A}\left\{\left(2+\frac{E_A}{E}\right)\ln\frac{2\left(\frac{m}{m^*}\right)\left[1+\sqrt{1-\frac{E_A}{E}\left(\frac{m}{m^*}-1\right)}\right]-\frac{E_A}{E}\left(\frac{m}{m^*}-1\right)}{2\left(\frac{m}{m^*}\right)\left[1-\sqrt{1-\frac{E_A}{E}\left(\frac{m}{m^*}-1\right)}\right]-\frac{E_A}{E}\left(\frac{m}{m^*}-1\right)}\right.$$
$$\left.-\left(1+\frac{m}{m^*}+\frac{E_A}{E}\right)\ln\frac{\left(\frac{m}{m^*}\right)^2+1+2\left(\frac{m}{m^*}\right)\sqrt{1-\frac{E_A}{E}\left(\frac{m}{m^*}-1\right)}-\frac{E_A}{E}\left(\frac{m}{m^*}-1\right)}{\left(\frac{m}{m^*}\right)^2+1-2\left(\frac{m}{m^*}\right)\sqrt{1-\frac{E_A}{E}\left(\frac{m}{m^*}-1\right)}-\frac{E_A}{E}\left(\frac{m}{m^*}-1\right)}\right\} \tag{9}$$

and

$$\sigma_{\rm em} = \frac{\pi}{3}(r_0\,\gamma)^2\,S\left(\frac{m}{m^*}\right)\frac{k_B\,T}{E_A}\left\{\left(2-\frac{E_A}{E}\right)\ln\frac{2\left(\frac{m}{m^*}\right)\left[1+\sqrt{1-\frac{E_A}{E}\left(\frac{m}{m^*}+1\right)}\right]+\frac{E_A}{E}\left(\frac{m}{m^*}+1\right)}{2\left(\frac{m}{m^*}\right)\left[1-\sqrt{1-\frac{E_A}{E}\left(\frac{m}{m^*}+1\right)}\right[+\frac{E_A}{E}\left(\frac{m}{m^*}+1\right)}\right.$$
$$\left.-\left(1-\frac{m}{m^*}-\frac{E_A}{E}\right)\ln\frac{\left(\frac{m}{m^*}\right)^2+1-2\left(\frac{m}{m^*}\right)\sqrt{1-\frac{E_A}{E}\left(\frac{m}{m^*}+1\right)}-\frac{E_A}{E}\left(\frac{m}{m^*}+1\right)}{\left(\frac{m}{m^*}\right)^2+1+2\left(\frac{m}{m^*}\right)\sqrt{1-\frac{E_A}{E}\left(\frac{m}{m^*}+1\right)}-\frac{E_A}{E}\left(\frac{m}{m^*}+1\right)}\right\}. \tag{10}$$

Since the simultaneous solution of Eqs. (8), (4) for small k is only possible for very small q the approximations leading to Eqs. (9), (10) are well justified. We observe that the cross sections vary as E in the vicinity of the limiting energies, while they vary as $1/E$ for neutron energies which are large in comparison with the limiting energies. A numerical evaluation of Eqs. (9), (10) is shown in Fig. 2.

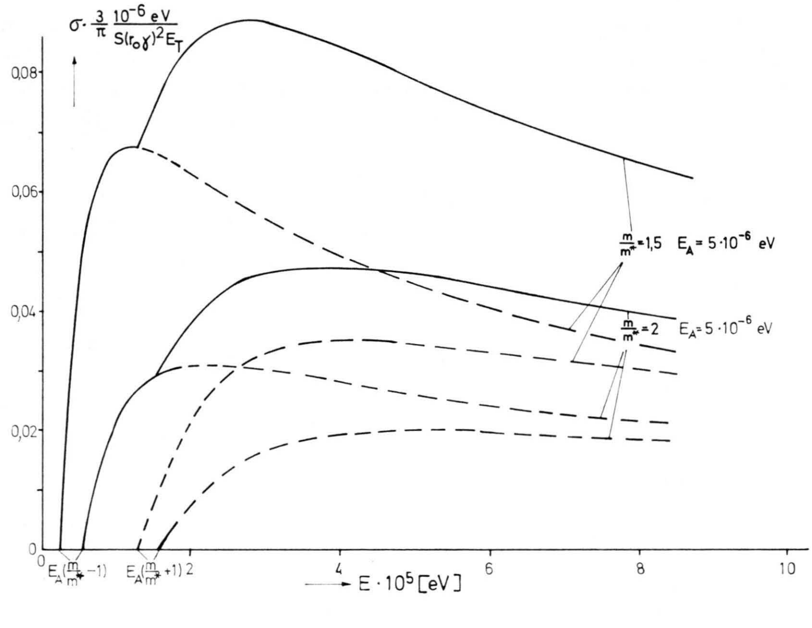

Fig. 2. Cross section of a weakly anisotropic ferromagnet at low temperatures plotted versus the neutron energy E. Solid lines: total cross sections, dashed lines: partial cross sections for magnon absorption and emission, respectively.

The cross section (suitably normalized) is plotted versus the neutron energy for two values of m/m^* ($E_T = k_B T$ thermal energy). The values of E_A and m/m^* can be taken from an experiment, if the positions of the two discontinuities in slope of the cross section are determined. This effect should be easily detectable for not two large m/m^* (i. e. substances with low critical temperatures). The finite linewidth of the spin waves has the tendency to smear out the discontinuities; this effect can be estimated to be very small if the temperatures are sufficiently low ($T \ll T_c$). It is to be expected that the present theory overestimates the magnitude of the observable cross sections, however: if E_A is very small the cross section diverges like $\ln 1/E_A$; in a real case the magnitude of the total cross section will be limited rather by the finite size of the magnetic domains than by the anisotropy energy. If a comparison with an actual experiment is made, an angular range around the forward direction according to the angular divergence of the incident neutron beam should be excluded from the angular integration leading to Eqs. (8), (10), since the differential cross section is very sharply peaked in the forward direction.

4. Critical Magnetic Scattering of Ultracold Neutrons

The spontaneous magnetization of a ferromagnet above the critical temperature T_c is zero, but the fluctuations of the local magnetization maintain spin correlations over distances, which are large compared to the atomic distances, for temperatures near T_c. According to VAN HOVE [20] the asymptotic behavior of the spin correlation function $\langle \mathbf{S}_0 \mathbf{S}_R \rangle$ is given by the Ornstein-Zernike function [21]

$$\langle \mathbf{S}_0 \mathbf{S}_R \rangle \xrightarrow[R\to\infty]{} \text{const}\ \frac{1}{R}\, e^{-\varkappa R}. \tag{11}$$

$\varkappa^{-1}$ range of the correlation (for $T \to T_c$ $\varkappa$ approaches zero). According to FISHER et al. [22] a parameter η has to be included

$$\langle \mathbf{S}_0 \mathbf{S}_R \rangle \xrightarrow[R\to\infty]{} \text{const}'\ \frac{1}{R^{1+\eta}}\, e^{-\varkappa R}. \tag{12}$$

The behavior of the correlation function for small values of distance R has been investigated using Monte Carlo techniques [23, 24]. The dynamical behavior of the fluctuations can be described by a spin diffusion law according to VAN HOVE [20] if large distances and large time intervals are considered. These spin fluctuations give rise to the critical scattering of neutrons. For small energy transfers $\hbar\,\omega$ and small momentum transfers the cross section is given by [20]

$$\frac{d^2\sigma}{d\Omega\, d\omega} = \frac{k'}{k}\,\frac{2}{3}\,(r_0\,\gamma)^2\, S(S+1)\, |F(\boldsymbol{q})|^2\, \chi(\boldsymbol{q})\, \frac{1}{\pi}\, \frac{\Gamma(\boldsymbol{q})}{\omega^2 + \Gamma^2(\boldsymbol{q})}. \tag{13}$$

The wave number dependent susceptibility $\chi(\boldsymbol{q})$ is derived by fourier transformation of the correlation function; according to the Ornstein-Zernike formula $\chi(\boldsymbol{q})$ is given by

$$\chi(\boldsymbol{q}) = \frac{1}{r_1^2}\,\frac{1}{\varkappa^2 + q^2}, \quad q < \varkappa, \tag{14}$$

r_1 parameter describing the range of the interaction and according to Fisher's theory

$$\chi(\boldsymbol{q}) = \frac{1}{r_1^{2-\eta}}\,\frac{1}{\left(\varkappa^2 + \frac{q^2}{1-\eta/2}\right)^{1-\eta/2}}, \quad q < \varkappa. \tag{15}$$

The concept of dynamic scaling [25–29] has to be taken into account to represent the linewidth $\Gamma(\boldsymbol{q})$ of the quasielastic scattering correctly. The results of the dynamic scaling hypothesis for the isotropic ferromagnet can be summarized by [29]

$$\Gamma(\boldsymbol{q}) = \Lambda\, q^2 \ \text{for}\ q \ll \varkappa, \qquad \Gamma(\boldsymbol{q}) = \Gamma_0\, q^{(5-\eta)/2}\ \text{for}\ q \gtrsim \varkappa. \tag{16}$$

Λ spin diffusion constant (from $\lim_{T\to T_c} \Gamma_0 \sim \lim_{T\to T_c} \Lambda \cdot \varkappa^{-(1-\eta)/2} \neq 0, \infty$ one immediately derives the relation between the critical exponents of Λ and $\varkappa$)

[20] L. VAN HOVE, Phys. Rev. **95**, 1374 [1954].
[21] L. S. ORNSTEIN and F. ZERNIKE, Proc. Acad. Sci. Amsterdam **17**, 793 [1914].
[22] M. E. FISHER and R. J. BURFORD, Phys. Rev. **156**, 583 [1967].
[23] K. BINDER and H. RAUCH, Z. Physik **219**, 201 [1969].
[24] K. BINDER and H. RAUCH, Z. Angew. Phys. **28**, 325 [1970].
[25] R. A. FERRELL, N. MENYHÁRD, H. SCHMIDT, F. SCHWABL, and P. SZÉPFALUSY, Phys. Rev. Lett. **18**, 891 [1967].
[26] K. KAWASAKI, J. Phys. Chem. Solids **28**, 1277 [1967].
[27] K. KAWASAKI, Progr. Theoret. Phys. **40**, 11, 706, 930 [1968].
[28] B. I. HALPERIN and P. C. HOHENBERG, Phys. Rev. Lett. **19**, 700 [1967].
[29] B. I. HALPERIN and P. C. HOHENBERG, Phys. Rev. **177**, 952 [1969].

In the hydrodynamic region ($q \ll \varkappa$) the behavior of the fluctuations is diffusive while in the transition region ($q \gtrsim \varkappa$) it is not. We use now the simplest model which is consistent with Eq. (16) to represent $\Gamma(\boldsymbol{q})$ for all values of q as indicated in Fig. 3. In the upper part of the figure the features

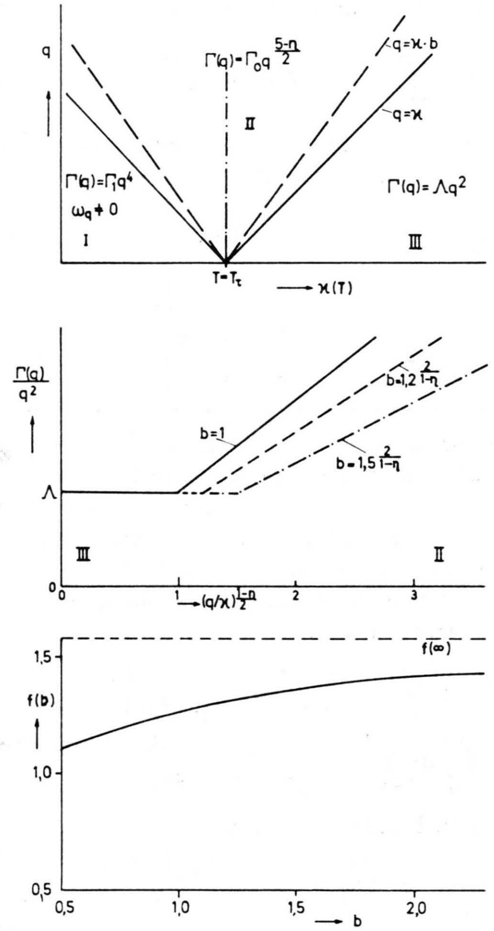

Fig. 3. Choice of the linewidth function $\Gamma(\mathbf{q})$ (middle part of the figure) according to the dynamical scaling assumptions (upper part of the figure). The lower part of the figure shows the resulting dependence of the cross section on the "boundary parameter" b. For explanations see the text.

of the dynamic scaling law are pointed out, while we plot the function which is used for the numerical calculations in the middle part of the figure. We define the constant Γ_0 by $\Gamma_0 = \Lambda(\varkappa\, b)^{-(1-\eta)/2}$, the boundary parameter b having the order of magnitude one. The sharp transition between the two regions for $q=\varkappa$ or $q=b\,\varkappa$, respectively, is a crude simplification, of course. The scattering of ultracold neutrons is predominantly hydrodynamic, however, since the neutron wavelengths are very large and the neutron energies are very small. The details of the model for large q affect the behavior of the cross section only slightly. Therefore we do not use the more sophisticated results which have been derived for $\Gamma(\boldsymbol{q})$ by use of mode-mode coupling theories [30–32] (and which do not agree with each other numerically). The behavior of $\chi(\boldsymbol{q})$ for large values of q has a small influence on the total cross section for the same reason. This is demonstrated explicitly by use of the mean field expression [16]

$$\chi^{-1}(\boldsymbol{q}) = \varkappa^2 + \frac{6}{d^2}\left[1 - \frac{1}{z}\sum \exp\{i\,\boldsymbol{q}\,\boldsymbol{R}\}\right] \quad (17)$$

(z number of nearest neighbours)

for the numerical calculations. We approximately average $\chi(\boldsymbol{q})$ over the directions by taking the average

$$\left\langle \frac{1}{z}\sum \exp\{i\,\boldsymbol{q}\,\boldsymbol{R}\}\right\rangle_{\Omega} = \frac{\sin q\,d}{q\,d}\,. \quad (18)$$

Using Eqs. (17), (18) instead of Eq. (14) for the numerical integrations changes the values of the total cross sections by less than 1% in the critical region; therefore the Eq. (14) or Eq. (15), respectively, are sufficient, and we need not consider the more complicated theories for the behavior of $\chi(\boldsymbol{q})$ for large q [22] (or, equivalently, the behavior of the correlations for small distances [23, 24]). The magnetic form factor is omitted for the same reason.

The result which we obtain for the total cross section depends now sensitively on the ratio $k/\varkappa$, i. e. the ratio of the correlation range to the neutron wavelength. If $k/\varkappa \ll 1$ we can neglect the Fisher parameter η since $\eta \ll 1$ and make the approximations

$$k'^2 = k^2 + \frac{2\,m\,\omega}{\hbar} \approx \frac{2\,m\,\omega}{\hbar}\,,$$
$$q^2 = k^2 + k'^2 - 2\,k\,k'\cos\vartheta \approx k'^2. \quad (19)$$

From Eq. (14) it is seen that typical values of the momentum transfer $\hbar\,q$ have the order of magnitude $\hbar\,\varkappa$, the energy transfer $\hbar\,\omega$ being large in comparison with the energy $\hbar^2 k^2/2\,m$ of the incident

[30] D. Huber and D. Krueger, Phys. Rev. Lett. **24**, 111 [1970].
[31] P. Résibois and C. Piette, Phys. Rev. Lett. **24**, 514 [1970].
[32] J. Villain, Internat. Conference on Magnetism, Grenoble 1970 (to be published).

neutrons. Therefore the approximations of Eq. (19) are justified, and we derive by straightforward integration the total cross section, which obeys a $1/v$-law

$$\sigma \cong \frac{16}{3}(r_0\gamma)^2 S(S+1)\frac{1}{r_1^2 k \varkappa}\Bigg\{\frac{\frac{2mA}{\hbar}}{1+\left(\frac{2mA}{\hbar}\right)^2}\arctan b + \frac{\frac{2mA}{\hbar\sqrt{k}}}{1+\left(\frac{2mA}{\hbar\sqrt{b}}\right)^4}$$
$$\cdot\Bigg[\frac{1}{\sqrt{2}}\left(1+\left(\frac{2mA}{\hbar\sqrt{b}}\right)\right)^2\left(\pi-\arctan(\sqrt{2b}-1)\;-\arctan(\sqrt{2b}+1)\right) \tag{20}$$
$$+\frac{1}{2\sqrt{2}}\ln\frac{b+\sqrt{2b}+1}{b-\sqrt{2b}+1}\left(1-\left(\frac{2mA}{\hbar\sqrt{b}}\right)^2\right)-\frac{2mA}{\hbar\sqrt{b}}\left(\pi-2\arctan\frac{2mA}{\hbar\sqrt{b}}\right)\Bigg]\Bigg\},\quad k\ll\varkappa.$$

The condition $k \ll \varkappa$ leads to the condition $2mA/\hbar \gg 1$ in practical cases, since the critical exponents of A and $\varkappa$ are related. Therefore we can write the cross section in the simpler form

$$\sigma \approx \frac{16}{3}(r_0\gamma)^2 S(S+1)\frac{1}{r_1^2 k\varkappa}\frac{1}{(2mA/\hbar)}f(b), \qquad k\ll\varkappa, \tag{21}$$

where the slowly varying function $f(b)$

$$f(b) = \arctan b + \sqrt{\frac{b}{2}}\left[\pi-\arctan(\sqrt{2b}-1)\;-\arctan(\sqrt{2b}+1)-\frac{1}{2}\ln\frac{b+\sqrt{2b}+1}{b-\sqrt{2b}+1}\right] \tag{22}$$

is plotted in the lower part of Fig. 3. Thus the cross section depends on the correlation range $\varkappa^{-1}$ and the spin diffusion constant A in a very simple way. It is interesting to note that the condition $2mA/\hbar \gg 1$ leading to Eq. (21) is valid for temperatures as close to the critical temperature as $(T-T_c/T_c)\approx 10^{-2}$ in the case of iron.

We have to calculate the cross section for arbitrary values of $k/\varkappa$ by numerical integration, suitably starting from the expression

$$\sigma = \frac{4}{3}(r_0\gamma)^2 S(S+1)\frac{1}{(k r_1)^{2-\eta}} I \tag{23}$$

with the dimensionless integral I

$$I = \int_0^\infty y\,dy\int_{(1-y)^2}^{(1+y)^2}\frac{dt}{\left[(\varkappa/k)^2+\frac{t}{1-\eta/2}\right]^{1-\eta/2}}\,\frac{\gamma(t)}{(y^2-1)^2+\gamma^2(t)} \tag{24}$$

with the notation according to Fig. 3

$$\gamma(t) = \begin{cases}\left(\dfrac{2mA}{\hbar}\right)t\left[\left(\dfrac{k}{\varkappa b}\right)^2 t\right]^{(1-\eta)/4} & \text{for } t > \left(\dfrac{\varkappa b}{k}\right)^2,\\[2ex] \left(\dfrac{2mA}{\hbar}\right)t & \text{for } t \leqq \left(\dfrac{\varkappa b}{k}\right)^2.\end{cases} \tag{25}$$

It can be verified explicitly that large values of y make only very small contributions to the integral Eq. (24) and therefore we write infinity for the upper limit. If $\varkappa \ll k$ the numerical integration in Eq. (24) has to be done with great care since the cross section is almost divergent. We now proceed to discuss the limiting value of the cross section for $\varkappa/k \to 0$. Using the notation $(2m\Gamma_0/\hbar)\cdot k^{(1-\eta)/2} = A$ we investigate the contribution of the divergence of the integrand separately

$$I = (1-\eta/2)^{(1-\eta/2)}\Bigg\{\int_0^{1-\varepsilon_0} y\,dy\int_{(1-y)^2}^{(1+y)^2}\frac{A\,t^{(1+\eta)/4}\,dt}{(y^2-1)^2+A^2 t^{(5-\eta)/2}}$$
$$+\int_{1+\varepsilon_0}^{\infty} y\,dy\int_{(1-y)^2}^{(1+y)^2}\frac{A\,t^{(1+\eta)/4}\,dt}{(y^2-1)^2+A^2 t^{(5-\eta)/2}} + J_1 \tag{26}$$

with $\varepsilon_0 \ll 1$ and the notation

$$J_1 = \int_{-\varepsilon_0}^{+\varepsilon_0}(1+\varepsilon)\,d\varepsilon\int_{\varepsilon^2}^{(2-\varepsilon)^2}\frac{A\,t^{(1+\eta)/4}\,dt}{4\varepsilon^2+4\varepsilon^3+\varepsilon^4+A^2 t^{(5-\eta)/2}}\,. \tag{27}$$

This integral can now be evaluated simply since $\varepsilon_0 \ll 1$ and for ultracold neutrons $A \lesssim 1$

$$J_1 \approx 2\int_0^{\varepsilon_0} d\varepsilon\int_{\varepsilon^2}^{4}\frac{A\,t^{(1+\eta)/4}\,dt}{4\varepsilon^2+A^2 t^{(5-\eta)/2}} \tag{28}$$
$$\approx \left(\frac{2}{A}\right)^{2\eta/(5-\eta)}\int_0^{\varepsilon_0}\frac{d\varepsilon}{\varepsilon^{1-2\eta/(5-\eta)}}\int_0^\infty\frac{x^{(1+\eta)/4}\,dx}{1+x^{(5-\eta)/2}}$$
$$\approx \frac{\pi}{\eta}\left(\frac{2\varepsilon_0}{A}\right)^{2\eta/(5-\eta)}.$$

Since $\eta \ll 1$ we can choose ε_0 suitable such that $J_1 \approx \pi/\eta$, the contributions of the first two integrals in Eq. (26) being negligible small in comparison with J_1. Therefore it is a reasonable approximation to replace the integral Eq. (26) by its limiting value for $\Lambda \to 0$, which can be calculated exactly using the representation of the δ-function

$$\lim_{x \to 0} \frac{x}{(y^2-1)^2+x^2} = \pi\,\delta(y^2-1) \tag{29}$$

yielding the result

$$\left.\begin{array}{r} \varkappa \to 0 \\ \dfrac{2\,m\,\Lambda}{\hbar} \to 0 \end{array}\right\} \quad \sigma = \frac{4\,\pi}{3}\,(r_0\,\gamma)^2\,S(S+1)\,\frac{1}{(k\,r_1)^{2-\eta}} \cdot \frac{2^\eta}{\eta}\,(1-\eta/2)^{(1-\eta/2)}\,. \tag{30}$$

The cross section at the critical temperature is thus inversely proportional to the critical exponent η. The cross section approaches this maximum value for $\varkappa \to 0$ as

$$\sigma \propto [1-(\varkappa/k)^\eta]/\eta \tag{31}$$

which is very similar to a logarithmic divergence $\sigma \propto \ln(k/\varkappa)$, however, since η is very small. It is not possible to derive η from experiments making use of Eq. (30), since this maximum value of the cross section will be reduced by the uncertainties in the temperature, temperature gradients, the finite size of the microdomains etc.

The results of the numerical evaluation of Eqs. (24), (25) are plotted in Fig. 4. The cross section (in dimensionless units) is plotted versus the ratio $\varkappa/k$ for different values of $2\,m\,\Lambda/\hbar$ and b. Curves for different values of η are practically identical (most of the curves given in the figure refer to $\eta = 0.0625$, a value being similar to the result of the threedimensional Ising model [22], and contain therefore no information about the limiting behavior Eq. (30), which is dashed-dotted drawn in the figure. We now use these general results to make some specific predictions about the temperature dependence of the cross sections for iron. We use the following choice of parameters

$$\begin{aligned} &\varkappa = \varkappa_0(1-T_c/T)^{0,650}\,, \\ &\Lambda = \Lambda_0(1-T_c/T)^{0,305}\,, \\ &\varkappa_0 = 0{,}855\ (\text{Å}^{-1}),\, 2\,m\,\Lambda_0/\hbar = 29{,}4 \end{aligned} \tag{32}$$

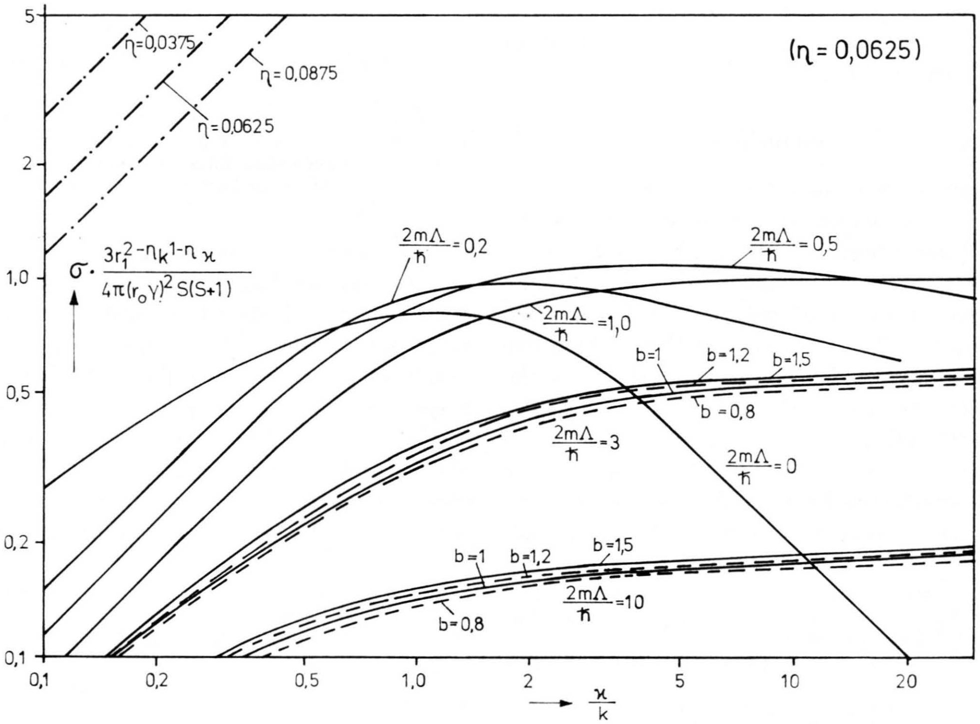

Fig. 4. Total magnetic cross sections plotted versus the ratio $\varkappa/k$. Curves for various values of Λ and b are shown (solid and dashed lines respectively). The dashed dotted straight lines represent the asymptotic ($\varkappa \to 0$ and $\Lambda \to 0$) behavior for different values of η.

which is consistent with the static [33] and dynamic [29] scaling laws, and yields parameters $\varkappa$, Λ having about the same order of magnitude as given by the experiments [34, 35] for $1 - T_c/T \approx 10^{-2}$. This choice is only a preliminary example, of course. There is much experimental disagreement about the spin diffusion constant and its temperature dependence [35–39]. The analysis of the energy distribution of the critically scattered cold neutrons is very difficult because of the angular range permitting hydrodynamic scattering shrinks to zero for $T \to T_c$. The experimental results on Λ have thus to be considered with some reservation [40]. Therefore the possibility of an indirect determination of the spin diffusion constant from the total cross section of ultracold neutrons may be of interest in some cases. In Fig. 5 we present the cross section as function of wave number k with the choice of parameters given by Eq. (32). The normalization of units is chosen in such a way that $1/v$-cross sections yield horizontal straight lines. Large deviations from the $1/v$-behavior are detectable when the critical temperature is approached. The dashed-dotted lines indicate the magnitude of the nuclear absorption cross section and the cross section given by lattice vibrations [41]. The magnetic scattering predominates in the vicinity of the critical temperature.

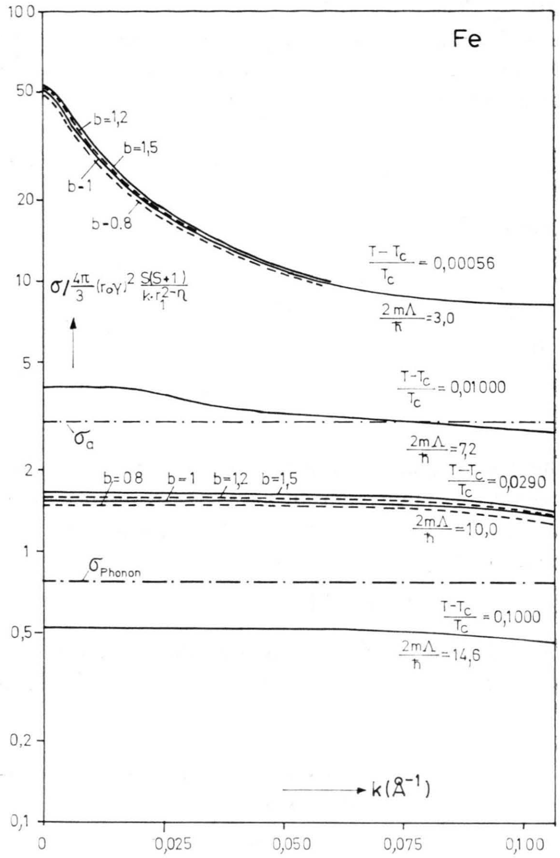

Fig. 5. Estimates for the total magnetic cross sections of iron as a function of neutron wave number k at various temperatures. The dashed-dotted lines represent the phonon cross section and the nuclear absorption cross section.

5. Conclusions

The characteristic properties of "ultracold" neutrons, large wavelength and small energy, can be very useful for neutron scattering investigations in solid state physics. This fact is demonstrated by some simple examples of magnetic scattering. We do not consider effects connected with the refractive index of neutrons which is very important for the slowest part of the ultracold neutron spectrum, since the refraction of the neutrons can be taken into account in a simple way [1, 2]. We first consider the Bragg scattering of ultracold neutrons from the vortex lattice in type II-superconductors. The advantages resulting from the large value of the cross section and the large Bragg angles are discussed. We then investigate the inelastic scattering from magnetic systems at low temperatures and at temperatures slightly above the critical temperature, respectively. We demonstrate that the total cross sections contain detailed information about the inelasticity of the scattering. Since we use very crude models to derive the cross sections, parts of the discussions may have preliminary character and a more

[33] L. P. KADANOFF, W. GÖTZE, D. HAMBLEN, R. HECHT, E. A. S. LEWIS, V. V. PALCIAUSKAS, M. RAYL, J. SWIFT, D. ASPNES, and J. KANE, Rev. Mod. Phys. **39**, 395 [1967].

[34] S. SPOONER and B. L. AVERBACH, Phys. Rev. **142**, 291 [1966].

[35] M. COLLINS, V. MINKIEVICZ, R. NATHANS, L. PASSELL, and G. SHIRANE, Phys. Rev. **179**, 417 [1969].

[36] B. JACROT, J. KONSTANTINOVIĆ, G. PARETTE, and D. CRIBIER, Inelastic Scattering of Neutrons in Solids and Liquids, IAEA, Vienna 1963, p. 317.

[37] L. PASSELL, K. BLINOWSKI, T. BRUN, and P. NIELSEN, Phys. Rev. **139**, A 1866 [1965].

[38] J. ALS-NIELSEN, Phys. Rev. Lett. **25**, 730 [1970].

[39] R. KAHN and G. PARETTE, International Conference on Magnetism, Grenoble 1970 (to be published).

[40] P. C. HOHENBERG, Varenna Lectures on Critical Phenomena, 1970, and private communication.

[41] K. BINDER, PTHM—FRM Nr. 110, 1970.

sophisticated reexamination may be necessary. We believe, however, that the main features of the scattering come out correctly from our simplified theory. Experiments are desirable to support this point. Since the dependence of the cross sections on the neutron velocity deviates from the simple $1/v$-behavior in a nontrivial way, a detailed analysis of measured neutron cross sections should be feasible. It is shown that the scattering by ferromagnetic spin waves in the vicinity of the forward direction allows conclusions concerning the anisotropy energy. The cross section for the critical scattering of ultracold neutrons is dominated by the parameters of the hydrodynamic theory, namely the range of the spin correlation $\varkappa^{-1}$ and the spin diffusion constant Λ. Remarkably large values for the magnitude of the cross sections are found. The survey of magnetic scattering treated in our paper is by no means complete, other topics are the critical scattering below the critical temperature, antiferromagnetic magnons, paramagnetic high-temperature diffusive scattering, inelastic spin-flip scattering by magnetic ions, critical magnetic scattering including anisotropy etc. It is clear, however, that in most of these cases more complicated models have to be used (for instance, see the dynamic scaling theory of anisotropic critical scattering given in [42]).

We add one remark about measurements of double differential cross sections, deriving $d^2\sigma/d\Omega\, d\omega$ with given accuracies Δq, $\Delta\omega$. From the intensity considerations in momentum space [43] it can be seen that the use of very cold neutrons may be favorable.

I want to express my gratitude to Dr. H. K. VONACH for suggesting this investigation and for stimulating discussions. I gratefully acknowledge useful discussions with Dr. A. STEYERL and the communication of his results prior to publication. I thank Dr. F. WEGNER for valuable discussions.

[42] F. WEGNER and E. RIEDEL, International Conference on Magnetism, Grenoble 1970 (to be published).

[43] H. MAIER-LEIBNITZ, Nukleonik **8**, 61 [1966].